Supporting Information

Efficient Electrocatalytic Conversion of N_2 to NH_3 on $NiWO_4$ Under Ambient Conditions

Jia Wang, [a‡] *Haeseong Jang,* [b‡] *Guangkai Li,* [a] *Min Gyu Kim,*[c] *Zexing Wu,* [a*] *Xien Liu* [a*] *and Jaephil Cho* [b*]

Dr. J. Wang, G. Li, Prof. Z. Wu, Prof. X. Liu
State Key Laboratory Base of Eco-chemical Engineering, College of Chemical Engineering, College of Chemistry and Molecular Engineering, Qingdao University of Science & Technology, Qingdao 266042, P. R. China
E-mail: splswzx@qust.edu.cn; liuxien@qust.edu.cn
Dr. H. Jang, Prof. J. Cho
Department of Energy Engineering School of Energy and Chemical Engineering Ulsan National Institute of Science and Technology (UNIST), Ulsan, 689-798, Korea
E-mail: jpcho@unist.ac.kr
Prof. M. Kim
Beamline Research Division, Pohang Accelerator Laboratory (PAL), Pohang 790-784, Korea.

List of Contents

electrolyte stained with NH_3 color agent before and after 1 h electrolysis at −0.3 V vs. RHE in N_2 atmosphere. (c) UV-Vis absorption spectra of the 0.1 M HCl electrolyte stained with NH_3 color agent before and after 1 h electrolysis at −0.3 V vs. RHE in Ar atmosphere. (d) UV-Vis absorption spectra of the 0.1 M HCl electrolyte stained with NH_3 color agent before and after 1h electrolysis at −0.3 V vs. RHE in N_2 atmosphere on the $NiWO_4$/CC electrode at open-circuit potential under ambient conditions.

Figure S6. (a) UV-Vis absorption spectra of various NH_3 concentrations after incubated for 1h at room temperature. (b) Calibration curve used for estimation of NH_3.

Figure S7. NH_3 yields and FE of different test numbers at -0.3 V after 1 h of electrolysis.

Figure S8. (a) XRD pattern of $NiWO_4$ after long-term stability measurement in 0.1 M HCl. High-resolution XPS spectra of Ni 2p (b), W 4f (c) and O 1s (d) after durability test.

Figure S9. SEM image of $NiWO_4$ after stability measurement in 0.1 M HCl (a) and corresponding EDS mappings of Ni (b), W (c) and O (d).

Figure S10 TEM image of $NiWO_4$ after stability measurement in 0.1 M HCl (a), (b), (c) and corresponding EDS mappings of Ni, W and O.

Figure S11 CV of $NiWO_4$ at N_2 or Ar in 0.1 M HCl (a) and 0.1 M Na_2SO_4 (b).

Figure S12 UV-Vis adsorption spectra of the electrolytes after 1 h electrolysis in Ar saturated solution at various potentials in 0.1 M HCl (a) and 0.1 M Na_2SO_4 (b).

Figure S13 UV-Vis adsorption spectra of the electrolytes after 1 h electrolysis in N_2 saturated solution without $NiWO_4$ at various potentials in 0.1 M HCl (a) and 0.1 M Na_2SO_4 (b)

Figure S14 UV-Vis adsorption spectra of the 0.1 M HCl electrolytes after 1 h electrolysis in N_2 saturated solution at various potentials.

Table S1. Comparison of the NH_3 electrosynthesis activity for $NiWO_4$ under ambient conditions with other catalysts.

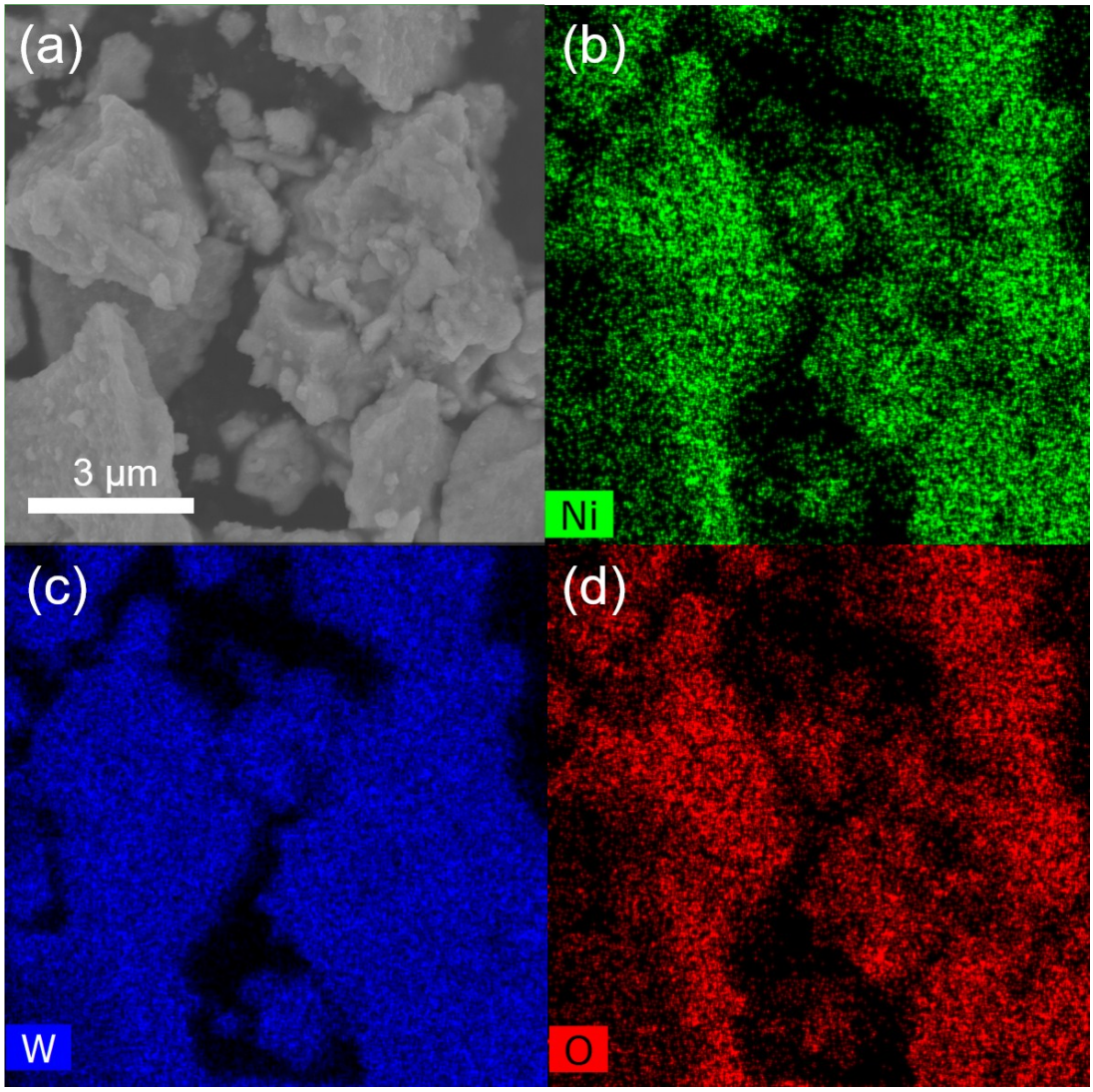

Figure S1. SEM image of $NiWO_4$ (a) and corresponding EDX mappings of Ni (b), W (c) and O (d).

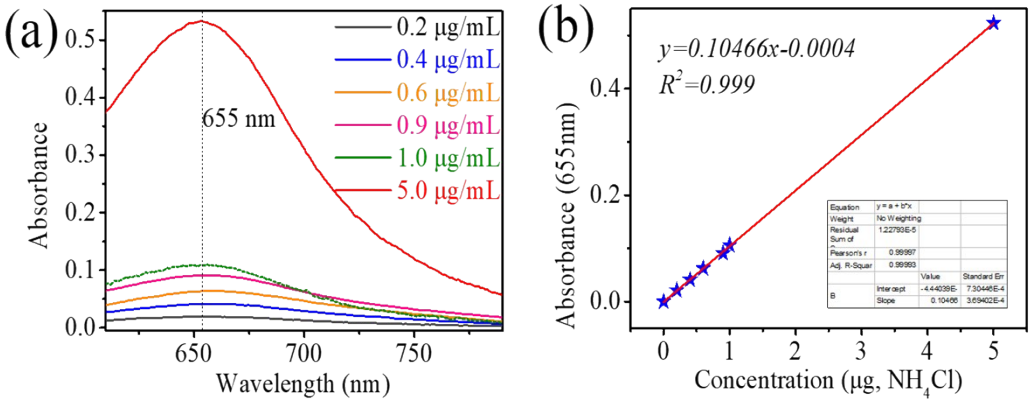

Figure S2. (a) UV-Vis absorption spectra of indophenol assays with NH_4^+ after incubated for 2 h at room temperature. (b) Calibration curve used for estimation of NH_4Cl.

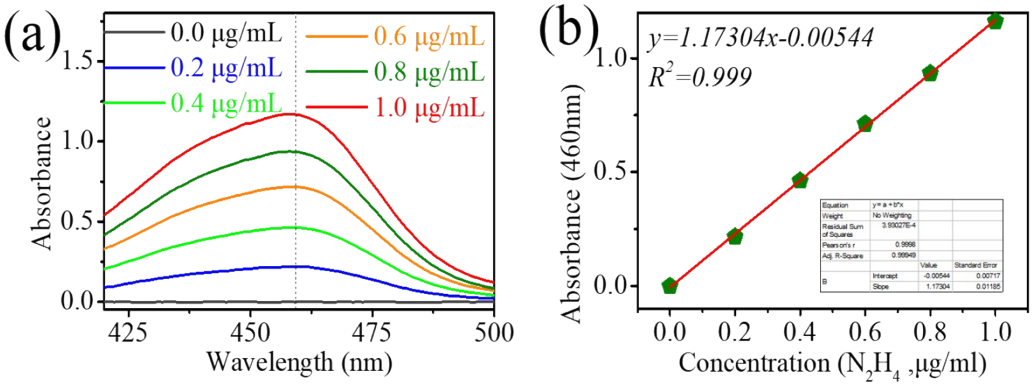

Figure S3. (a) UV-Vis absorption spectra of various N_2H_4 concentrations after incubated for 10 min at room temperature. (b) Calibration curve used for calculation of N_2H_4 concentrations.

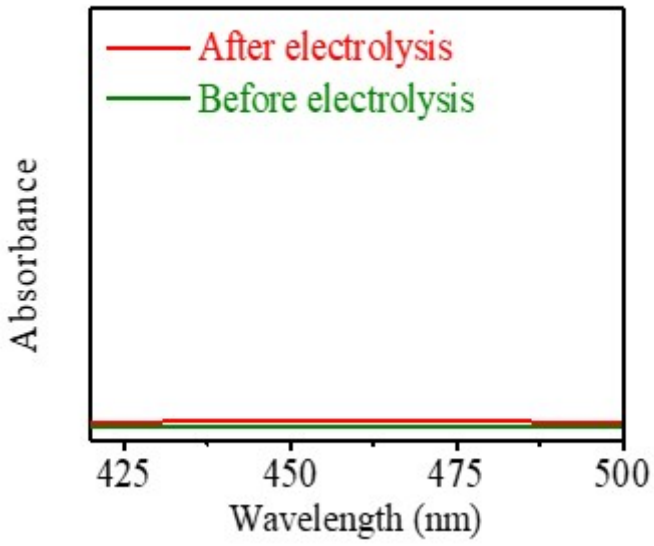

Figure S4. UV-Vis absorption spectra of the 0.1 M HCl electrolyte (after charging at −0.3 V vs. RHE for 1 h) after incubated for 10 min at room temperature.

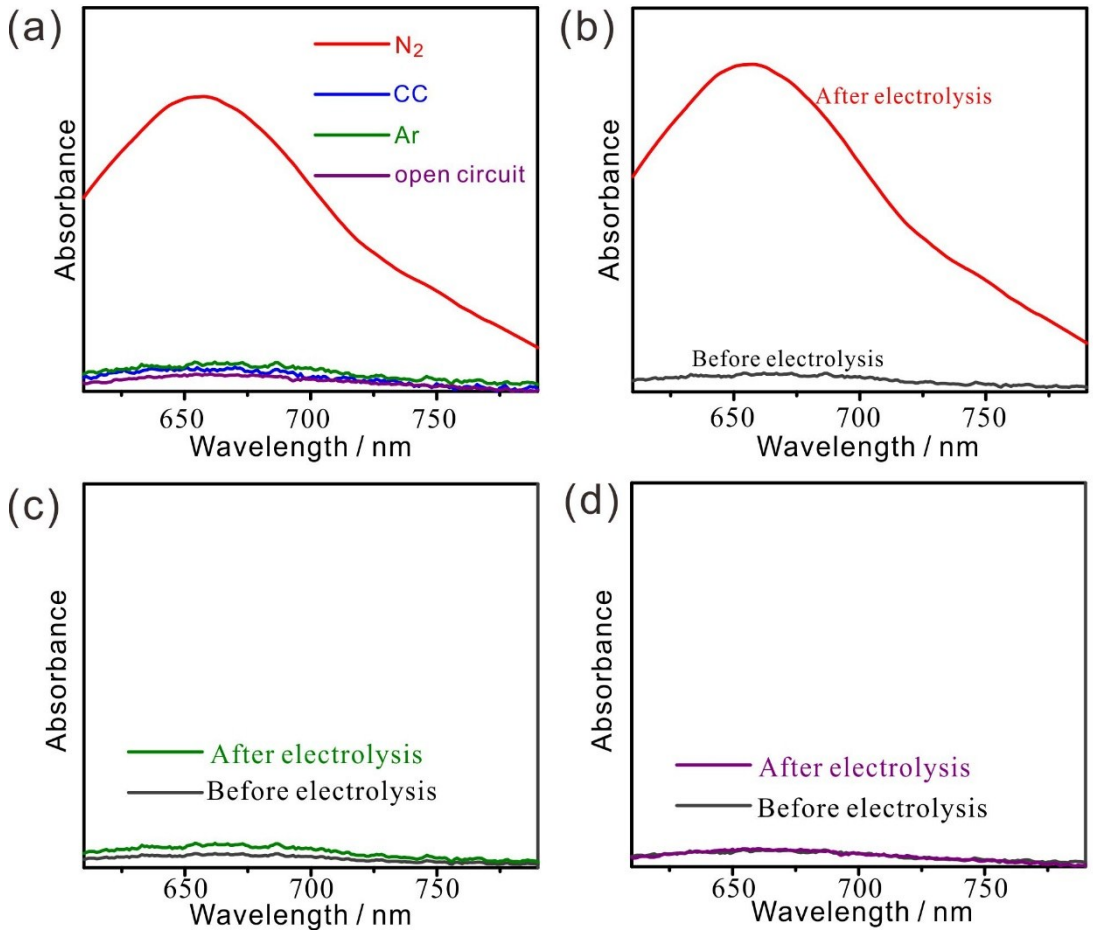

Figure S5. (a) UV-Vis absorption spectra of the electrolytes coloured with indophenol indicator after charging at -0.3 V for 1 h in different conditions. (b) UV-Vis absorption spectra of the 0.1 M HCl electrolyte stained with NH_3 color agent before and after 1 h electrolysis at −0.3 V vs. RHE in N_2 atmosphere. (c) UV-Vis absorption spectra of the 0.1 M HCl electrolyte stained with NH_3 color agent before and after 1 h electrolysis at −0.3 V vs. RHE in Ar atmosphere. (d) UV-Vis absorption spectra of the 0.1 M HCl electrolyte stained with NH_3 color agent before and after 1h electrolysis at −0.3 V vs. RHE in N_2 atmosphere on the $NiWO_4$/CC electrode at open-circuit potential under ambient conditions.

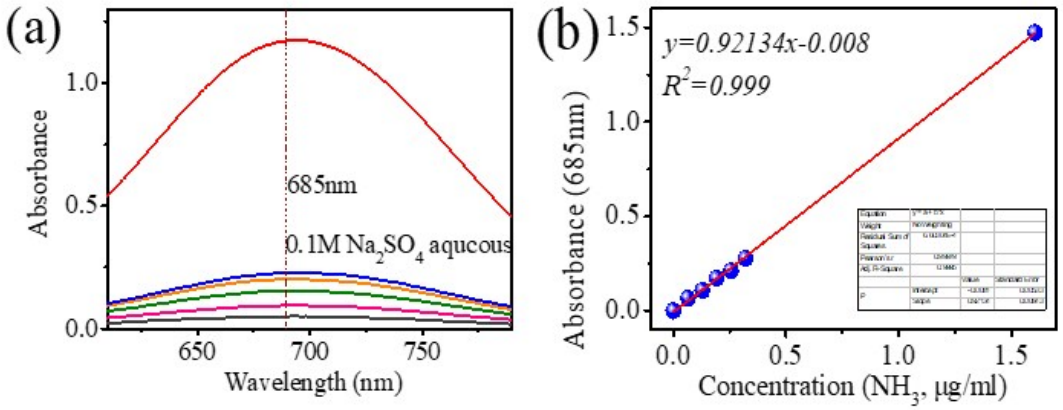

Figure S6. (a) UV-Vis absorption spectra of various NH_3 concentrations after incubated for 1h at room temperature. (b) Calibration curve used for estimation of NH_3.

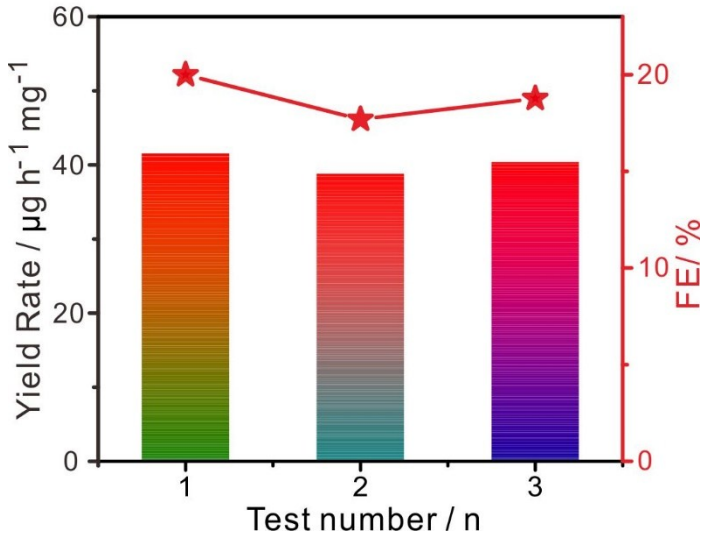

Figure S7. NH_3 yields and FE of different test numbers at -0.3 V in 0.1 M HCl after 1 h of electrolysis.

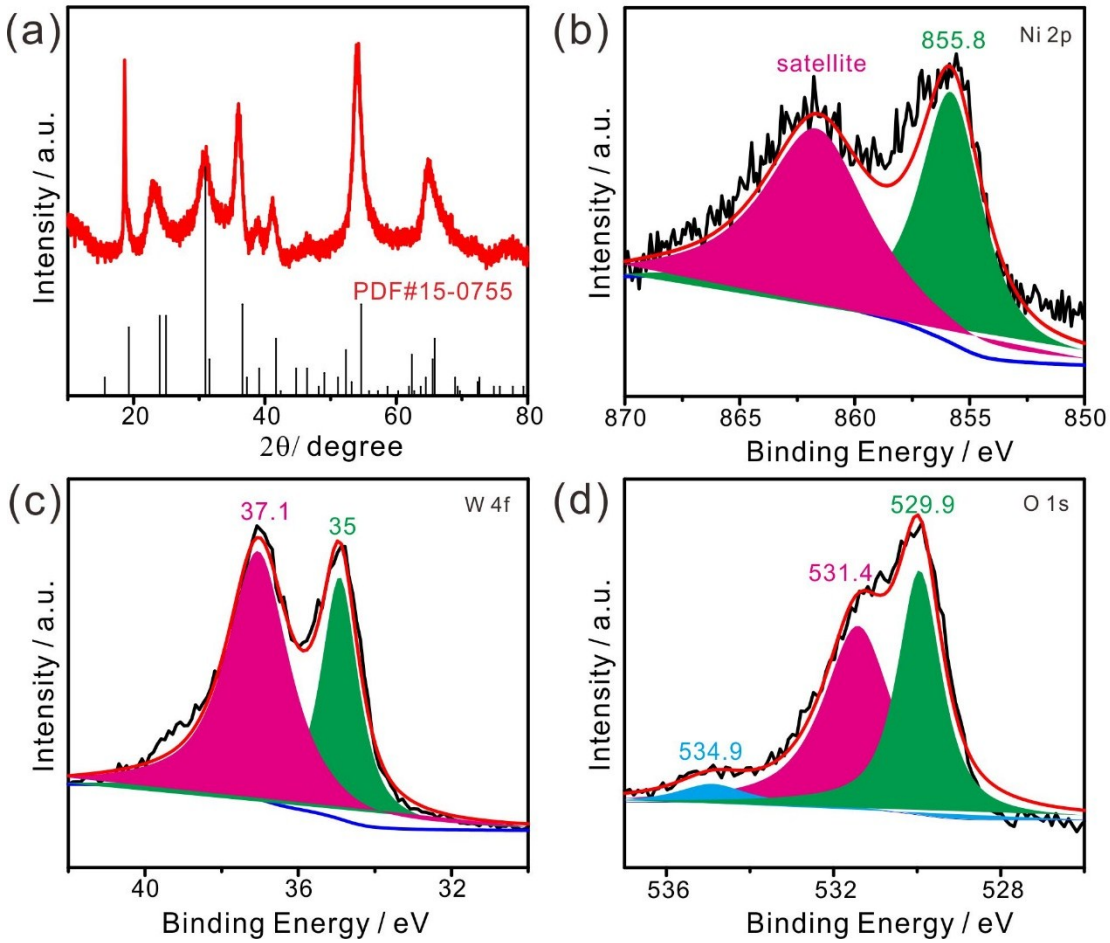

Figure S8. (a) XRD pattern of $NiWO_4$ after long-term stability measurement in 0.1 M HCl. High-resolution XPS spectra of Ni 2p (b), W 4f (c) and O 1s (d) after durability test.

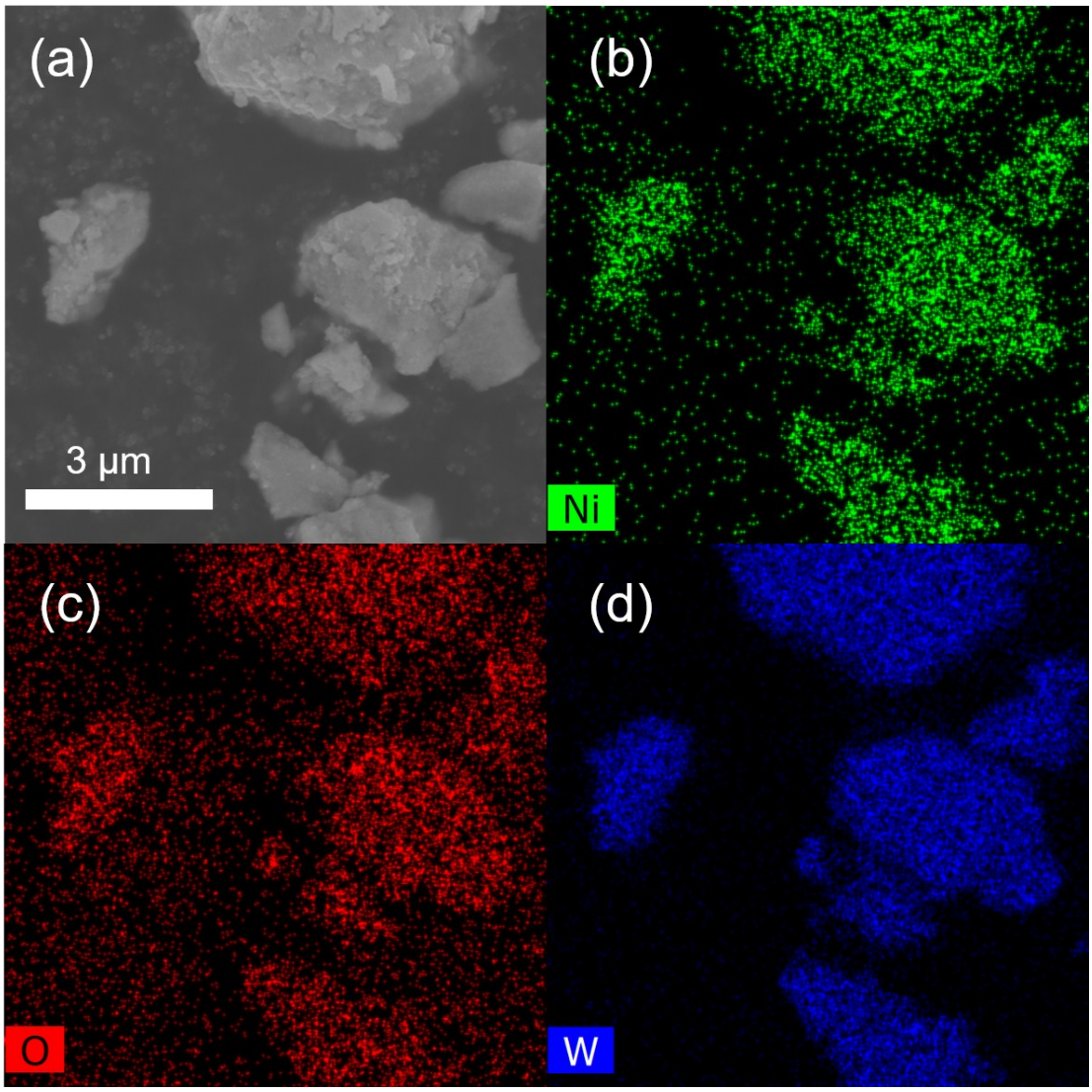

Figure S9. SEM image of $NiWO_4$ after stability measurement in 0.1 M HCl (a) and corresponding EDS mappings of Ni (b), W (c) and O (d).

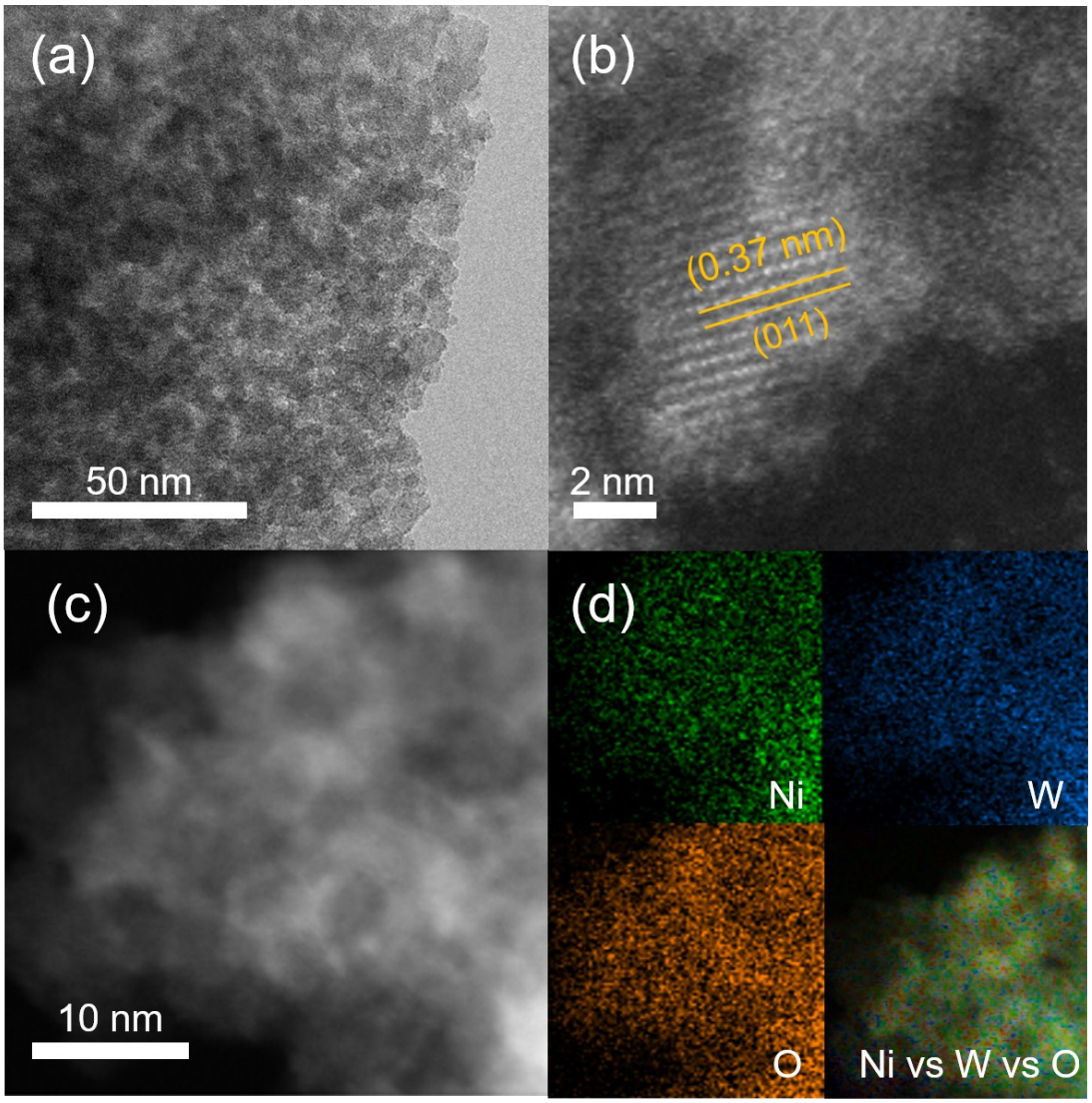

Figure S10 TEM image of $NiWO_4$ after stability measurement in 0.1 M HCl (a), (b), (c)and corresponding EDS mappings of Ni, Wand O.

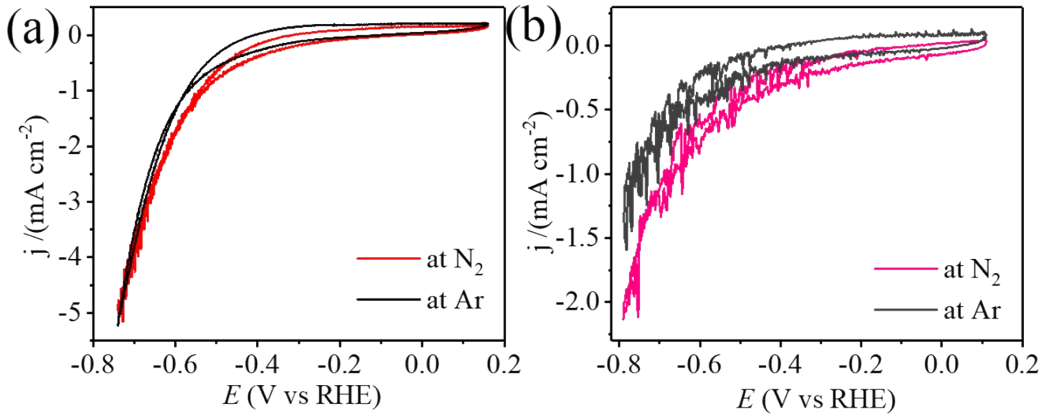

Figure S11 CV of $NiWO_4$ at N_2 or Ar in 0.1 M HCl (a) and 0.1 M Na_2SO_4 (b).

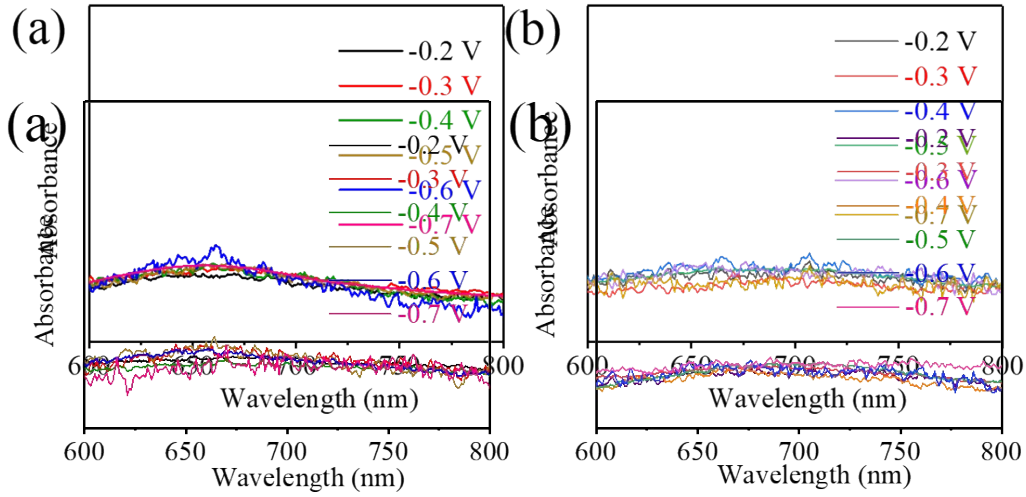

Figure S12 UV-Vis adsorption spectra of the electrolytes after 1 h electrolysis in Ar saturated solution at various potentials in 0.1 M HCl (a) and 0.1 M Na_2SO_4 (b)

Figure S13 UV-Vis adsorption spectra of the electrolytes after 1 h electrolysis in N_2 saturated solution without $NiWO_4$ at various potentials in 0.1 M HCl (a) and 0.1 M Na_2SO_4 (b).

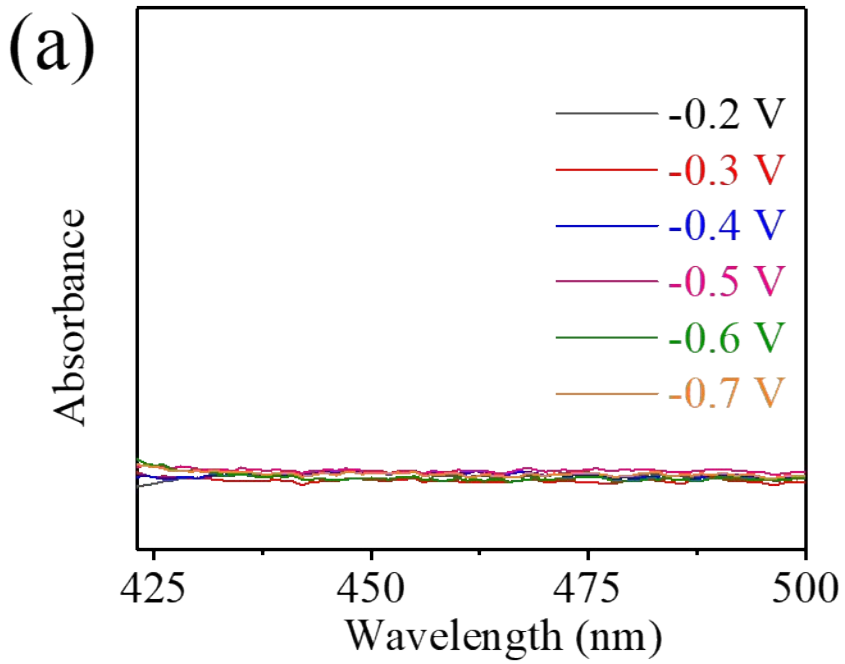

Figure S14 UV-Vis adsorption spectra of the 0.1 M HCl electrolytes after 1 h electrolysis in N_2 saturated solution at various potentials.

Table S1. Comparison of the NH_3 electrosynthesis activity for $NiWO_4$ under ambient conditions with other catalysts.

Catalyst	Electrolyte	NH_3 Yield Rate	FE (%)	NH_4^+-N Testing Method	Ref
$NiWO_4$	0.1M HCl 0.1M Na_2SO_4	48.86 μg h^{-1} mg^{-1} 28.4 μg h^{-1} mg^{-1}	19.32 10.18	Indophenol method	This Work
Sn/SnS_2	0.1M PBS	23.8 μg h^{-1} mg^{-1}	6.5	Indophenol method	[1]
W_2N_3	0.1M HCl	11.66 μg h^{-1} mg^{-1}	11.67	Indophenol method	[2]
Ru_{SAs}/N-C	0.05M H_2SO_4	120.9 μg h^{-1} mg^{-1}	29.6	Indophenol method	[3]
pAu/NF	0.1M Na_2SO_4	9.42 μg h^{-1} cm^{-2}	13.36	Indophenol method	[4]
BiNCs	0.5M K_2SO_4	200 mmol g^{-1} h^{-1}	66	Nessler's reagent	[5]
Bi NS	0.1M Na_2SO_4	13.23 μg h^{-1} mg^{-1}	10.46	Indophenol method	[6]
$FeS@MoS_2$/CFC	0.1M Na_2SO_4	8.45 μg h^{-1} cm^{-2}	2.96	Indophenol method	[7]
$N@MoS_2$	0.1M Na_2SO_4	69.82 μg h^{-1} mg^{-1}	9.14	Indophenol method	[8]
$Fe@Fe_3O_4$	0.2M $NaHCO_3$	7.956 μg h^{-1} cm^{-2}	6.25	Nessler's reagent	[9]
Mn_3O_4	0.1M Na_2SO_4	11.6 μg h^{-1} mg^{-1}	3	Indophenol method	[10]
AuNPs	0.1M Li_2SO_4	9.22 μg h^{-1} cm^{-2}	73.32	Indophenol method	[11]
Fe_{SA}-N-C	0.1M KOH	7.48 μg h^{-1} mg^{-1}	56.55	Indophenol method	[12]
O-MoC@NC	0.5M Li_2SO_4	22.5 μg h^{-1} mg^{-1}	25.1	Indophenol method	[13]
p-Fe_2O_3/CC	0.1M Na_2SO_4	13.56 μg h^{-1} mg^{-1}	7.69	Indophenol method	[14]
Ag_3Cu BPNs	0.1M Na_2SO_4	24.59 μg h^{-1} mg^{-1}	13.28	Indophenol method	[15]
PC/Sb/$SbPO_4$	0.1M HCl	25 μg h^{-1} mg^{-1}	31	Indophenol method	[16]
Mo_2C/C	0.5 m Li_2SO_4	11.3 μg h^{-1} mg^{-1}	7.8	Nessler's reagent	[17]
Fe-TiO_2	0.5M $LiClO_4$	25.47 μg h^{-1} mg^{-1}	25.6	Indophenol method	[18]

Eex-COF/NC	0.1M KOH	12.53 μg h^{-1} mg^{-1}	45.43	Indophenol method	[19]
BCC PdCu	0.5M LiCl	35.7 μg h^{-1} mg^{-1}	11.5	Indophenol method	[20]

References

[1] P. Li, W. Fu, P. Zhuang, Y. Cao, C. Tang, A. B. Watson, P. Dong, J. Shen, M. Ye, *Small,* 2019, **15**, e1902535.

[2] H. Jin, L. Li, X. Liu, C. Tang, W. Xu, S. Chen, L. Song, Y. Zheng, S. Z. Qiao, *Adv. Mater.,* 2019, **31**, e1902709.

[3] Z. Geng, Y. Liu, X. Kong, P. Li, K. Li, Z. Liu, J. Du, M. Shu, R. Si, J. Zeng, *Adv. Mater.,* 2018, **40**, 1803498.

[4] H. Wang, H. Yu, Z. Wang, Y. Li, Y. Xu, X. Li, H. Xue, L. Wang, *Small*, 2019, **15**, e1804769.

[5] Y.-C. Hao, Y. Guo, L.-W. Chen, M. Shu, X.-Y. Wang, T.-A. Bu, W.-Y. Gao, N. Zhang, X. Su, X. Feng, J.-W. Zhou, B. Wang, C.-W. Hu, A.-X. Yin, R. Si, Y.-W. Zhang, C.-H. Yan, *Nat. Catal.,* 2019, **2**, 448-456.

[6] L. Li, C. Tang, B. Xia, H. Jin, Y. Zheng, S.-Z. Qiao, *ACS Catal.*, 2019, **9**, 2902-2908.

[7] Y. Guo, Z. Yao, B. J. J. Timmer, X. Sheng, L. Fan, Y. Li, F. Zhang, L. Sun, *Nano Energy,* 2019, **62**, 282-288.

[8] L. Zeng, S. Chen, J. van der Zalm, X. Li, A. *Chen, Chem. Commun (Camb)*, 2019, **55**, 7386-7389.

[9] C. Li, Y. Fu, Z. Wu, J. Xia, X. Wang, *Nanoscale*, 2019, **11**, 12997-13006.

[10] X. Wu, L. Xia, Y. Wang, W. Lu, Q. Liu, X. Shi, X. Sun, *Small,* 2018, **14**, e1803111.

[11] L. Tan, N. Yang, X. Huang, L. Peng, C. Tong, M. Deng, X. Tang, L. Li, Q. Liao, Z. Wei, *Chem. Commun (Camb),* 2019, 55, 14482-14485.

[12] M. Wang, S. Liu, T. Qian, J. Liu, J. Zhou, H. Ji, J. Xiong, J. Zhong, C. Yan, *Nat. Comm.,* 2019, **10**, 341.

[13] X. Qu, L. Shen, Y. Mao, J. Lin, Y. Li, G. Li, Y. Zhang, Y. Jiang, S. Sun, *ACS Appl. Mater. Inter*., 2019, **11**, 31869-31877.

[14] Z. Wang, K. Zheng, S. Liu, Z. Dai, Y. Xu, X. Li, H. Wang, L. Wang, *ACS Sustainable Chem. Eng.,* 2019, **7**, 11754-11759.

[15] H. Yu, Z. Wang, D. Yang, X. Qian, Y. Xu, X. Li, H. Wang, L. Wang, *J. Mater. Chem. A,* 2019, **7**, 12526-12531.

[16] X. Liu, H. Jang, P. Li, J. Wang, Q. Qin, M. G. Kim, G. Li, J. Cho, *Angew. Chem. Int. Ed.,* 2019, **58**, 13329-13334.

[17] H. Cheng, L. X. Ding, G. F. Chen, L. Zhang, J. Xue, H. Wang, *Adv. Mater.,* 2018, **30**, e1803694.

[18] T. Wu, X. Zhu, Z. Xing, S. Mou, C. Li, Y. Qiao, Q. Liu, Y. Luo, X. Shi, Y. Zhang, X. Sun, *Angew. Chem. Int. Ed.,* 201911153.

[19] S. Liu, M. Wang, T. Qian, H. Ji, J. Liu, C. Yan, *Nat. Comm.,* 2019, **10**, 3898.

[20] X. Huang, *Angew. Chem. Int. Ed.,* 201913122.